FEBS openbio

FEBS PRESS science publishing by scientists

Human nitrobindin: the first example of an all-β-barrel ferric heme-protein that catalyzes peroxynitrite detoxification

Giovanna De Simone[1], Alessandra di Masi[1], Fabio Polticelli[1,2] and Paolo Ascenzi[3]

1 Department of Sciences, Roma Tre University, Italy
2 National Institute of Nuclear Physics, Roma Tre Section, Italy
3 Interdepartmental Laboratory for Electron Microscopy, Roma Tre University, Italy

Keywords
human nitrobindin; kinetics; peroxynitrite scavenging; protection of L-tyrosine nitration

Correspondence
P. Ascenzi, Interdepartmental Laboratory for Electron Microscopy, Roma Tre University, Via della Vasca Navale 79, I-00146 Roma, Italy
Fax: +39 06 57336321
Tel: +39 06 57333621
E-mail: ascenzi@uniroma3.it

(Received 14 August 2018, revised 29 August 2018, accepted 26 September 2018)

doi:10.1002/2211-5463.12534

Nitrobindins (Nbs), constituting a heme-protein family spanning from bacteria to *Homo sapiens*, display an all-β-barrel structural organization. Human Nb has been described as a domain of the nuclear protein named THAP4, whose physiological function is still unknown. We report the first evidence of the heme-Fe(III)-based detoxification of peroxynitrite by the all-β-barrel *C*-terminal Nb-like domain of THAP4. Ferric human Nb (Nb (III)) catalyzes the conversion of peroxynitrite to NO_3^- and impairs the nitration of free L-tyrosine. The rate of human Nb(III)-mediated scavenging of peroxynitrite is similar to those of all-α-helical horse heart and sperm whale myoglobin and human hemoglobin, generally taken as the prototypes of all-α-helical heme-proteins. The heme-Fe(III) reactivity of all-β-barrel human Nb(III) and all-α-helical prototypical heme-proteins possibly reflects the out-to-in-plane transition of the heme-Fe(III)-atom preceding peroxynitrite binding. Human Nb(III) not only catalyzes the detoxification of peroxynitrite but also binds NO, possibly representing a target of reactive nitrogen species.

In living organisms, all-α-helical globins (e.g., hemoglobin (Hb) and myoglobin (Mb)) play pivotal roles in ligand (e.g., O_2) transport, storage, and sensing, as well as in heme-Fe-based catalysis [1–7]. Most of them display the classical 3/3 globin fold, which is made up by six α-helices facing the heme; the A, B, and E α-helices form one face of the sandwich, the other side being built by the F, G, and H α-helices [1,3,4,7–9]. Recently, the 2/2 subset of the classical 3/3 α-helical fold was discovered; it is a sort of bundle composed of antiparallel pairs, the α-helices B/E and G/H sandwiching the heme [10,11]. In all-α-helical globins, the heme is deeply buried in the protein matrix contacting several hydrophobic residues that prevent the oxidation of the metal center [1,3–5,7,11]. The fifth coordination ligand of the heme-Fe atom is invariantly the side chain of the proximal HisF8 residue [1,3,4,7]. The heme distal ligand is represented generally by the E7 residue (mostly His and Tyr), which contributes to the modulation of the metal center reactivity and the stability of the heme-bound ligand [1,3,4,7,12–17].

Over the last two decades, monomeric all-β-barrel heme-proteins have been reported. They include *Rhodnius prolixus* nitrophorins (NPs) [18–21], and nitrobindins (Nbs), spanning from bacteria to *H. sapiens* [21–24]. Furthermore, the mixed α-helical-β-barrel

Abbreviations
Cj-trHbP, *Campylobacter jejuni* truncated hemoglobin P; CL-cyt*c*, cardiolipin-bound cytochrome *c*; CM-cyt*c*, carboxymethylated cytochrome *c*; Hb, hemoglobin; human Nb(III), ferric *Cj*-trHbP; human SA-heme, human serum heme-albumin; *Ma*-Pgb, *Methanosarcina acetivorans* protoglobin; Mb, myoglobin; *Mt*-trHbN, *Mycobacterium tuberculosis* truncated hemoglobin N; Nb(III), ferric Nb; Nb, nitrobindin; NONOate, 1,1-diethyl-2-hydroxy-2-nitroso-hydrazine; NP, nitrophorin; *Ph*-trHbO, *Pseudoalteromonas* haloplanktis truncated hemoglobin O.

heme-proteins human α1-microglobulin and *Cimex lectularius* NP have been described [21,25–27]. Nbs display a ten-stranded antiparallel β-barrel fold in which the penta-coordinated heme-Fe atom is secured to the protein by the proximal His residue [21–24,27]. In Nbs, the heme is highly solvent exposed and is stable in the ferric form, allowing to bind NO [21–24]. Interestingly, human Nb has been described as a domain of the nuclear protein named THAP4 whose function is still unknown [21,23,24]. THAP4 is composed of 567 amino acids and consists of an N-terminal modified zinc finger domain that binds DNA and the *C*-terminal Nb(III) domain [23,28,29].

Here, the first evidence of the heme-Fe-based detoxification of peroxynitrite by the ferric all-β-barrel *C*-terminal Nb(III) domain of THAP4 (hereafter human Nb(III)) is reported. Human Nb(III) catalyzes efficiently the conversion of peroxynitrite to NO_3^- and impairs the peroxynitrite-mediated nitration of free L-tyrosine. These results point to a role of THAP4 in reactive nitrogen species chemistry.

Materials

The pReceiver-B03 vector containing the transcript variant 2 of *H. sapiens* Nb(III) domain (GeneCopoeia, Rockville, MD, USA) was used to amplify by PCR the Nb gene (fw_HindIII_NdeI: 5′-GCCCAAGCTTCATATGGAGCC CCCCAAG-3′ and rv_BamHI: 5′-CGCGGATCCTTACGG GGTCAC-3′). The fragment of 500 bp was first subcloned in the pBluescript KS(−) and finally cloned in the pET-28a (+) vector. The *Escherichia coli* BL21(DE3) strain was used to express the 6 × His-tag-Nb in the presence of 0.2 mM δ-aminolevulinic acid. The expression of the 6 × His-tagged Nb was induced by adding 1 mM isopropyl-β-d-thiogalactoside for 16 h at 37 °C. The bacterial pellet was lysed in 20 mM phosphate buffer pH 7.5, 140 mM NaCl, and 0.015% Tween-20, and the supernatant was loaded onto a His-Trap affinity chromatography column (GE Healthcare Bio-Sciences, Amersham, UK). The adsorbed 6 × His-tag-Nb was eluted by a linear gradient of imidazole (20 mM phosphate buffer pH 7.4, 500 mM NaCl, and 10–1000 mM imidazole). The fractions containing the fusion protein were dialyzed against 20 mM phosphate buffer, pH 7.4, and analyzed by western blot using the primary anti-6 × His-tag antibody (Thermo Fisher Scientific, Waltham, MA, USA). The human Nb(III) concentration was determined spectrophotometrically by the pyridine hemochromogen method [30]. Human apo-Nb was prepared by the acid–acetone method [30].

Peroxynitrite was purchased from Cayman Chemical (Ann Arbor, MI, USA). The concentration of peroxynitrite was determined spectrophotometrically prior to each experiment by measuring the absorbance at 302 nm ($\varepsilon = 1.705 \times 10^3\ M^{-1}\cdot cm^{-1}$) [31]. L-Tyrosine, nitro-L-tyrosine, and 1,1-diethyl-2-hydroxy-2-nitroso-hydrazine (NONOate) were obtained from Sigma-Aldrich (St. Louis, MO, USA). All the other chemicals were purchased from Merck KGaA (Darmstadt, Germany). All chemicals were of analytical grade and were used without further purification.

Methods

Peroxynitrite isomerization by human Nb(III) and apo-Nb was investigated by rapid mixing the human Nb(III) or apo-Nb solutions (final concentration ranging between 5.0×10^{-6} and 3.5×10^{-5} M) with the peroxynitrite solution (final concentration, 2.0×10^{-4} M). Kinetics were recorded by using the SFM-20/MOS-200 rapid-mixing stopped-flow apparatus (BioLogic Science Instruments, Claix, France) monitoring absorbance changes at 302 nm [31]; the light path of the observation chamber was 10 mm, and the dead-time was 1.3 ms. In agreement with literature data [31,32], the absorbance at 302 nm decreased upon mixing the human Nb(III) and peroxynitrite solutions, reflecting the isomerization of peroxynitrite. No absorbance spectroscopic changes were observed in the Soret region in the course of the human Nb(III)-mediated isomerization of peroxynitrite.

Kinetics of peroxynitrite isomerization by human Nb (III) and apo-Nb were analyzed in the framework of the reaction scheme shown in Fig. 1 [31–46].

Values of the pseudo-first-order rate constant for peroxynitrite isomerization in the presence of human Nb(III) and human apo-Nb (i.e., k_{obs}) were determined from the analysis of the time-dependent absorbance decrease at 302 nm, according to Eqn (1) [36–46]:

$$[\text{peroxynitrite}]_t = [\text{peroxynitrite}]_i \times e^{-k_{obs} \times t} \quad (1)$$

Values of the second-order rate constant for peroxynitrite isomerization by human Nb(III) (i.e., k_{on}) and of the first-order rate constant for the spontaneous decay of peroxynitrite (i.e., k_0) were obtained from the dependence of k_{obs} on the ferric heme-protein concentration (i.e., [human Nb(III)], according to Eqn (2) [36–46]:

$$k_{obs} = k_{on} \times [\text{human Hb(III)}] + k_0 \quad (2)$$

The effect of pH on values of k_{on} and k_0 for peroxynitrite isomerization was analyzed according to Eqn (3) [36,38,39,46–48]:

$$k = (k_{lim} \times 10^{-pH})/(10^{-pH} + 10^{-pKa}) \quad (3)$$

where k is either k_{obs} or k_0 and k_{lim} represents the top asymptotic value of k under conditions where $pH \ll pK_a$.

The reaction of peroxynitrite with free L-tyrosine was carried out at pH 7.1 and 25.0 °C by adding 0.2 mL of an alkaline (1.0×10^{-3} M NaOH), ice-cooled solution of peroxynitrite (2.0×10^{-3} M) to 1.8 mL of a buffered

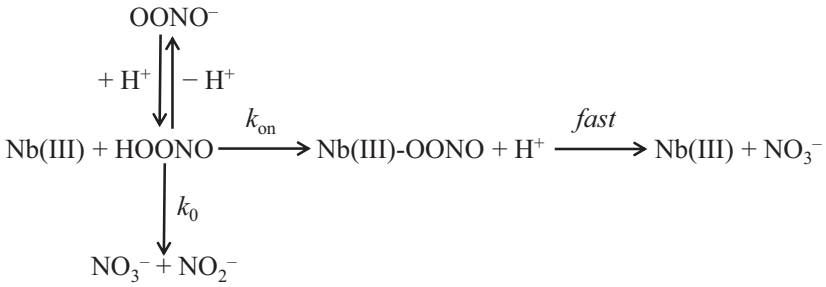

Fig. 1. Peroxynitrite isomerization in the absence and presence of human Nb(III).

(5.0×10^{-2} M phosphate buffer) solution of L-tyrosine (final concentration, 1.0×10^{-4} M) in the absence and presence of human Nb(III) and apo-Nb (final concentration, 3.5×10^{-5} M). The amount of nitro-L-tyrosine was determined by HPLC analysis [36–39,46].

The NO_2^- and NO_3^- concentrations were determined spectrophotometrically at 543 nm by using the Griess reagent and VCl_3 to catalyze the conversion of NO_3^- to NO_2^- [36,39,49]. The samples were prepared by mixing 0.5 mL of either a human Nb(III) or an apo-Nb solution (final concentration, 3.5×10^{-5} M in 5.0×10^{-2} M phosphate buffer, pH 7.1) with 0.5 mL of a peroxynitrite solution (final concentration, 2.0×10^{-4} M in 1.0×10^{-2} M NaOH) while vortexing, at 25.0 °C. The reaction mixture was analyzed within 10 min according to literature [36,39,49].

The absorbance spectrum of nitrosylated human Nb(III) was obtained by adding NONOate (1.0×10^{-4}) M to human Nb(III) (3.5×10^{-6} M).

Kinetic data were analyzed using the MATLAB program (The MathWorks Inc., Natick, MA, USA). The results are given as mean values of at least four experiments plus and minus the standard deviation.

Results and Discussion

Under all the experimental conditions, most of the time course of peroxynitrite isomerization (from 92% to 100%) was fitted to a single-exponential decay according to Eqn (1; Fig. 2, panel A). In fact, < 10% of the initial part of the time course of peroxynitrite isomerization was lost in the dead-time of the rapid-mixing stopped-flow apparatus, depending on the decomposition rate.

The pseudo-first-order rate constant for human Nb (III)-mediated isomerization of peroxynitrite (i.e., k_{obs}) increases linearly with the protein concentration (Fig. 2, panel B). This suggests that (a) the formation of the transient human Nb(III)-OONO species represents the rate-limiting step in catalysis, and (b) the conversion of human Nb(III)-OONO to Nb(III) and NO_3^- and NO_2^- is faster than human Nb(III)-OONO formation by at least 10-fold. The analysis of the data shown in Fig. 2 (panel B), according to Eqn (2), allowed us to determine the values of the second-order rate constant for peroxynitrite isomerization by human Nb(III) (i.e., k_{on}, corresponding to the slope of the linear plots) and of the first-order rate constant for the spontaneous peroxynitrite isomerization (i.e., k_0, corresponding to the *y*-intercept of the linear plots) (Table 1). Values of k_0 here determined agree with those previously reported [32,36–42,45,46].

To confirm the role of the heme-Fe(III) atom in catalysis, values of k_{obs} have been determined in the presence of human apo-Nb, which does not catalyze the peroxynitrite isomerization. Indeed, values of k_{obs} obtained in the presence of human apo-Nb correspond to those of k_0 (Fig. 2, panel C) as reported, among others, for horse heart apo-Mb and human apo-Hb [36].

In the presence of human Nb(III), the values of the relative yield of NO_3^- and NO_2^- for the isomerization of peroxynitrite are 89 ± 2% and 12 ± 1%. However, in the absence of human Nb(III) and in the presence of human apo-Nb, the values of the relative yield of NO_3^- and NO_2^- are 68 ± 3% and 31 ± 2%, and 71 ± 2% and 28 ± 3%, respectively. These data well agree with those reported for peroxynitrite isomerization by ferric heme-proteins such as horse heart apo-Mb and human apo-Hb [36].

The pH dependence of k_{on} and k_0 values for peroxynitrite isomerization allowed us to identify tentatively the species that preferentially react(s) with the heme-Fe(III) atom. Values of k_{on} and k_0 increase upon decreasing pH (Fig. 3, panels A and B). The pK_a values for the pH dependence of k_{on} and of k_0 are 6.7 ± 0.2 and 6.8 ± 0.2, respectively (Fig. 3). The pK_a values here determined agree well with those previously reported for the heme-protein-mediated isomerization of peroxynitrite [31,33,39,45,46].

The close similarity of the pH dependence of k_{on} for the human Nb(III)-mediated isomerization of peroxynitrite (Fig. 3, panel A) and of k_0 for peroxynitrite isomerization in the absence of human Nb(III) (Fig. 3, panel B) suggests that the HOONO species (Fig. 1)

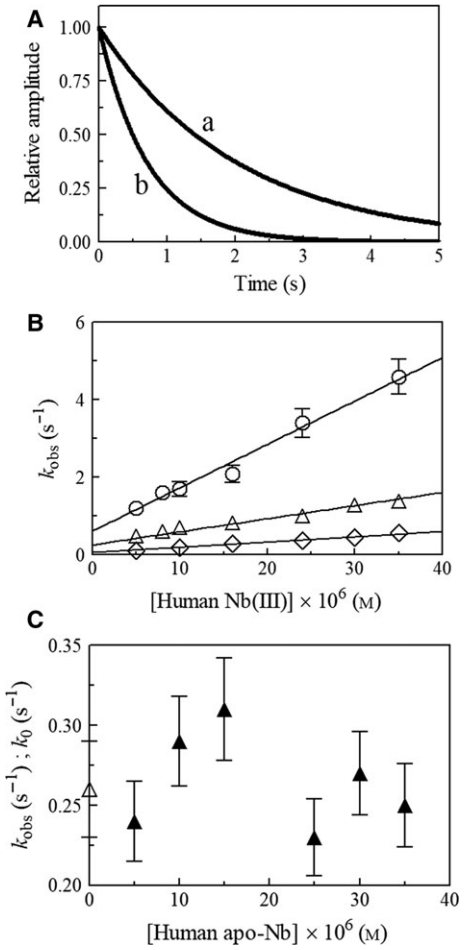

Fig. 2. Effect of human Nb(III) on peroxynitrite isomerization (k_{obs}), at 25.0 °C. (A) Averaged time courses of the human Nb(III)-mediated isomerization of peroxynitrite at pH 7.1. Data analysis according to Eqn (1) allowed us to determine the following values of k_{obs}: 4.9 × 10^{-1} s^{-1} (trace a) and 1.4 s^{-1} (trace b). The human Nb(III) concentration was 5.0 × 10^{-6} M (trace a) and 3.5 × 10^{-5} M (trace b). The peroxynitrite concentration was 2.0 × 10^{-4} M. (B) Dependence of k_{obs} on the human Nb(III) concentration, at pH 6.1 (open circles), 7.1 (open triangles), and 7.7 (open diamonds). Kinetics were analyzed according to Eqn (2) with values of k_{obs} and k_0 given in Table 1. (C) Dependence of k_{obs} on the human apo-Nb concentration, at pH 7.1. The symbol on the ordinate axis indicates the value of k_0 (=(2.6 ± 0.3) × 10^{-1} s^{-1}). The average value of k_{obs} is (2.7 ± 0.4) × 10^{-1} s^{-1}. The peroxynitrite concentration was 2.0 × 10^{-4} M. Where not shown, the standard deviation is smaller than the symbol.

reacts preferentially with the heme-Fe(III) atom [31,33,38,46]. Since the absorbance spectrum of Nb (III) is unaffected by pH over the whole range explored (i.e., between pH 6.1 and 7.7; Fig. S1), it is unlikely that values of k_{on} (Fig. 3, panel A) are affected by the acid–base equilibrium(a) of the ferric heme-protein.

Table 1. Values of k_{on} and k_0 values for peroxynitrite isomerization by human Nb(III), at 25.0 °C.

pH	k_{on} (M^{-1}·s^{-1})	k_0 (s^{-1})
6.1	(1.1 ± 0.1) × 10^5	(6.2 ± 0.7) × 10^{-1}
6.3	(9.8 ± 1.1) × 10^4	(4.9 ± 0.5) × 10^{-1}
6.6	(8.1 ± 0.8) × 10^4	(4.1 ± 0.4) × 10^{-1}
7.1	(3.4 ± 0.4) × 10^4	(2.6 ± 0.3) × 10^{-1}
7.4	(1.8 ± 0.2) × 10^4	(1.3 ± 0.1) × 10^{-1}
7.7	(1.3 ± 0.2) × 10^4	(6.3 ± 0.8) × 10^{-2}

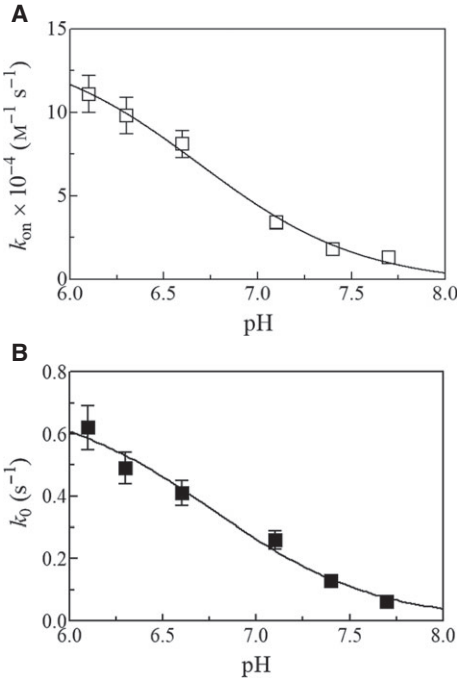

Fig. 3. Effect of pH on human Nb(III)-mediated peroxynitrite isomerization, at 25.0 °C. (A) Effect of pH on values of k_{on}. The continuous line was calculated according to Eqn (3) with pK_a = 6.7 ± 0.2 and k_{lim} = (1.4 ± 0.1) × 10^5 M^{-1}·s^{-1}. (B) Effect of pH on values of k_0. The continuous line was calculated according to Eqn (3) with pK_a = 6.8 ± 0.2 and k_{lim} = (7.1 ± 0.5) × 10^{-1} s^{-1}. Where not shown, the standard deviation is smaller than the symbol.

To analyze the protective role of human Nb(III) against peroxynitrite-mediated nitration, the relative yield of nitro-L-tyrosine formed by the reaction of peroxynitrite with free L-tyrosine in the absence and presence of human Nb(III) and apo-Nb was determined. As expected, human Nb(III) protects dose-dependently free L-tyrosine against peroxynitrite-mediated nitration, whereas L-tyrosine nitration is not prevented by human apo-Nb (Fig. 4).

The value of k_{on} for peroxynitrite isomerization by all-β-barrel human Nb(III) is similar to that of most

ferric all-α-helical globins (i.e., *Methanosarcina acetivorans* protoglobin (*Ma*-Pgb), *Mycobacterium tuberculosis* truncated hemoglobin N (*Mt*-trHbN), *Pseudoalteromonas haloplanktis* truncated hemoglobin O (*Ph*-trHbO), horse heart Mb(III), sperm whale Mb (III), human Hb(III), human serum heme-albumin (human SA-heme), and *Fusarium oxysporum* cytochrome P450 NO reductase) and mixed β-barrel/α-helical cardiolipin-bound and carboxymethylated cytochrome *c* (CL-cyt*c* and CM-cyt*c*, respectively) (Table 2) ([33,36–44] and present study), suggesting that neither the very different structural organization [1,3,22,23,50–58] nor the different solvent and ligand accessibility to the metal center (Fig. 5, panel A) ([1,3,22,23,50–58] and present study) nor the Lewis acidity of the heme-Fe(III) atom [38] are at the root of the modulation of peroxynitrite isomerization. In fact, the reactivity of these heme-proteins appears to be limited by the out-to-in-plane movement of the heme-Fe(III) atom preceding ligand (i.e., peroxynitrite) binding (Fig. 5, panel B). Of note, in ferric all-β-barrel human Nb and in most all-α-helical globins (e.g., sperm whale Mb and human Hb), the heme-Fe(III) atom is positioned ~ 0.35 to ~ 0.65 Å out-of-plane on the proximal side with respect to the pyrrole nitrogen atoms of the porphyrin, respectively (Fig. 5, panel B) ([1,3,22,23,50–54,57,58] and present study). The high reactivity of ferric *Campylobacter jejuni* truncated hemoglobin P (*Cj*-trHbP) (Table 2) reflects the high ligand accessibility to the heme center by the HisE7 path, the dynamic balance of hydrogen-bonding interactions at the heme distal site, and the penta-coordination of the heme-Fe atom; this suggested a role of *Cj*-trHbP in performing a peroxidase-like chemistry [46,59–61]. Furthermore, peroxynitrite isomerization by penta-coordinated sterically open heme-model compounds (Table 2) could reflect the in- or out-of-plane position of the heme-Fe(III) atom on the proximal side with respect to the pyrrole nitrogen atoms of the macrocycle [34,35,45].

Human Nb(III) not only catalyzes the detoxification of peroxynitrite but also binds reversibly NO (Fig. S1), as already reported for *Arabidopsis thaliana* Nb [22]. In fact, upon mixing human Nb(III) and NONOate solutions, the maximum of the absorbance spectrum of human Nb(III) shifts from 406 nm (human Nb(III)) to

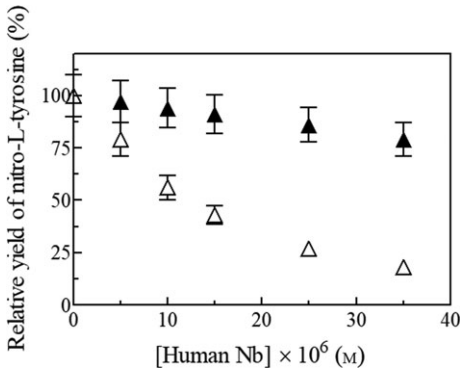

Fig. 4. Protective role of Nb on peroxynitrite-mediated nitrosylation of free L-tyrosine, at pH 7.1 and 25.0 °C. Effect of human Nb(III) (open triangles) and apo-Nb (filled triangles) concentration on the relative yield of nitro-L-tyrosine formed by the reaction of peroxynitrite with free L-tyrosine. The symbol on the ordinate axis (open triangle) indicates the relative yield of nitro-L-tyrosine obtained in the absence of human Nb(III) and apo-Nb. The free L-tyrosine concentration was 1.0×10^{-4} M. The peroxynitrite concentration was 2.0×10^{-4} M. Relative nitro-L-tyrosine yield (%) = (yield with added human Nb(III) or apo-Nb/yield with no human Nb(III) or apo-Nb) × 100. Where not shown, the standard deviation is smaller than the symbol.

Table 2. Peroxynitrite scavenging by ferric heme-proteins and heme-model compounds. n.d., not determined.

Heme-protein	k_{on} ($M^{-1} \cdot s^{-1}$)	k_0 (s^{-1})
Methanosarcina acetivorans Pgb[a]	3.8×10^4	2.8×10^{-1}
Mycobacterium tuberculosis trHbN[b]	6.2×10^4	2.7×10^{-1}
Pseudoalteromonas haloplanktis-trHbO[c]	2.9×10^4	2.8×10^{-1}
Campylobacter jejuni-trHbP [d]	9.6×10^5	3.0×10^{-1}
Horse heart Mb[e]	2.9×10^4	3.5×10^{-1}
Sperm whale Mb[f]	1.6×10^4	n.d.
Human Hb[e]	1.2×10^4	3.0×10^{-1}
Human Nb[g]	3.4×10^4	2.6×10^{-1}
Human SA-heme[h]	4.1×10^5	2.6×10^{-1}
CL-cyt*c*[i]	3.2×10^5	2.9×10^{-1}
CM-cyt*c*[i]	6.8×10^4	2.8×10^{-1}
Fusarium oxysporum cytochrome P450 NO reductase[k]	$\sim 5 \times 10^5$	9.0×10^{-2}
Fe(TMPS)[l]	6.0×10^4	5.5×10^{-1}
Fe(TMPS)[m]	3.0×10^5	1.35
Fe(TPPS)[m]	8.6×10^5	1.35
Fe(TMPyP)[m]	1.6×10^6	1.35
MP11[n]	4.1×10^4	2.8×10^{-1}

[a] pH 7.4 and 20.0 °C. From [44].
[b] pH 7.0 and 20.0 °C. From [42].
[c] pH 7.0 and 20.0 °C. From [43].
[d] pH 7.3 and 25.0 °C. From [46].
[e] pH 7.0 and 20.0 °C. From [36].
[f] pH 7.5 and 20.0 °C. From [38].
[g] pH 7.1 and 25.0 °C. Present study.
[h] pH 7.2 and 22.0 °C. From [39].
[i] pH 7.0 and 20.0 °C. CL was 1.6×10^{-4} M. From [40].
[j] pH 7.0 and 20.0 °C. From [41].
[k] pH 8.0 and 12.0 °C. From [33].
[l] pH 7.6 and 25.0 °C. From [34].
[m] pH 7.4 and 37.0 °C. From [35].
[n] pH 7.2 and 20.0 °C. From [45].

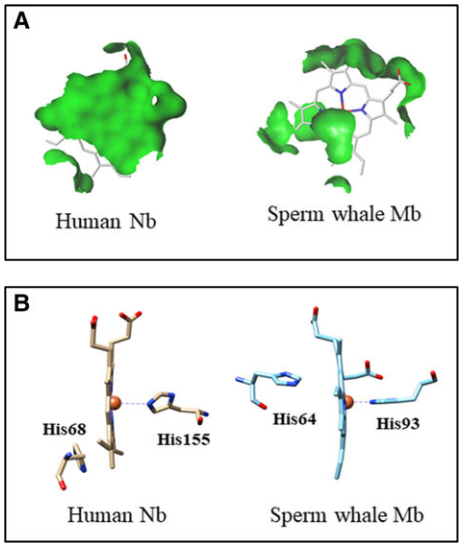

Fig. 5. Structural aspects of the heme site of human Nb(III) (PDB code: 3IA8) [23] and sperm whale Mb(III) (PDB code: 5MBN) [50]. (A) Solvent accessible surface of the heme distal site of human Nb (III) and sperm whale Mb(III). The heme distal plane is much more solvent accessible in human Nb(III) than in sperm whale Mb(III). (B) Schematic representation of the heme coordination in human Nb (III) and sperm whale Mb(III). The heme proximal residues of human Nb and sperm whale Mb are His155 and His93, respectively. In human Nb(III) and sperm whale Mb(III), the heme-Fe(III) atom is positioned ~ 0.35 and ~ 0.65 Å out-of-plane on the proximal side with respect to the pyrrole nitrogen atoms of the porphyrin, respectively. The pictures have been drawn with UCSF-Chimera package [64].

412 nm (human Nb(III)-NO). Moreover, human Nb (III)-NO can be converted to human Nb(III) by pumping off NO.

In light of these considerations, data here reported highlight for the first time the capability of the Nb-like domain of human THAP4 protein to catalyze peroxynitrite scavenging, to impair the peroxynitrite-mediated nitration of free L-tyrosine, and to bind NO. Considering the structural organization of THAP4 [23,28,29], it can be speculated that THAP4 may play a role in the chemistry of reactive nitrogen species by coupling the heme-based Nb reactivity with the modulation of genes transcription. This somehow resembles other heme-proteins like NPAS2, in which the heme redox status controls NPAS heterodimerization with BMAL1 and, in turn, DNA binding and target gene expression [62,63]. Similar to *A. thaliana* Nb [22], human Nb is firmly in the ferric form possibly distinguishing among NO, CO, and O_2. In fact, human Nb (III) selectively binds NO without recognizing CO and O_2 that are typical diatomic gaseous ligands of ferrous metal centers.

We are presently working on the functional analysis of the full-length human THAP4 protein as well as of its N- and/or C-terminal deleted forms to understand the molecular mechanisms underpinning THAP4 cellular functions.

Acknowledgements

The grant of Excellence Departments, MIUR, Italy (Articolo 1, Commi 314-337, Legge 232/2016), is gratefully acknowledged.

Author contributions

GDS performed the experiments and analyzed data. AM performed the comparative analysis of data. FP contributed to analyze the results and to draft the paper. PA coordinated the study and wrote the paper.

Conflict of interest

The authors declare no conflict of interest.

References

1 Perutz MF (1979) Regulation of oxygen affinity of hemoglobin: influence of structure of the globin on the heme iron. *Annu Rev Biochem* **48**, 327–386.
2 Bunn HF and Forget BG (1986) *Hemoglobin: Molecular, Genetic and Clinical Aspects*. Saunders WB Company, Philadelphia.
3 Bolognesi M, Bordo D, Rizzi M, Tarricone C and Ascenzi P (1997) Nonvertebrate hemoglobins: structural bases for reactivity. *Prog Biophys Mol Biol* **68**, 29–68.
4 Frauenfelder H, McMahon BH and Fenimore PW (2003) Myoglobin: the hydrogen atom of biology and a paradigm of complexity. *Proc Natl Acad Sci USA* **100**, 8615–8617.
5 Smith LJ, Kahraman A and Thornton JM (2010) Heme proteins - diversity in structural characteristics, function, and folding. *Proteins* **78**, 2349–2368.
6 Girvan HM and Munro AW (2013) Heme sensor proteins. *J Biol Chem* **288**, 13194–13203.
7 Ascenzi P and Brunori M (2016) A molecule for all seasons: the heme. *J Porphyrins Phthalocyanines* **20**, 134–149.
8 Domingues-Hamdi E, Vasseur C, Fournier JB, Marden MC, Wajcman H and Baudin-Creuza V (2014) Role of α-globin H helix in the building of tetrameric human hemoglobin: interaction with α-hemoglobin stabilizing protein (AHSP) and heme molecule. *PLoS ONE* **9**, e111395.
9 Vasseur C and Baudin-Creuza V (2015) Role of alpha-hemoglobin molecular chaperone in the hemoglobin formation and clinical expression of some hemoglobinopathies. *Transfus Clin Biol* **22**, 49–57.

10 Pesce A, Couture M, Dewilde S, Guertin M, Yamauchi K, Ascenzi P, Moens L and Bolognesi M (2000) A novel two-over-two α-helical sandwich fold is characteristic of the truncated hemoglobin family. *EMBO J* **19**, 2424–2434.
11 Pesce A, Bolognesi M and Nardini M (2013) The diversity of 2/2 (truncated) globins. *Adv Microb Physiol* **63**, 49–78.
12 Kitagawa T, Ondrias MR, Rousseau DL, Ikeda-Saito M and Yonetani T (1982) Evidence for hydrogen bonding of bound dioxygen to the distal histidine of oxycobalt myoglobin and haemoglobin. *Nature* **298**, 869–271.
13 Olson JS, Mathews AJ, Rohlfs RJ, Springer BA, Egeberg KD, Sligar SG, Tame J, Renaud JP and Nagai K (1988) The role of the distal histidine in myoglobin and haemoglobin. *Nature* **336**, 265–266.
14 Perutz MF (1989) Myoglobin and haemoglobin: role of distal residues in reactions with haem ligands. *Trends Biochem Sci* **14**, 42–44.
15 Rohlfs RJ, Mathews AJ, Carver TE, Olson JS, Springer BA, Egeberg KD and Sligar SG (1990) The effects of amino acid substitution at position E7 (residue 64) on the kinetics of ligand binding to sperm whale myoglobin. *J Biol Chem* **265**, 3168–3176.
16 Brantley RE Jr, Smerdon SJ, Wilkinson AJ, Singleton EW and Olson JS (1993) The mechanism of autooxidation of myoglobin. *J Biol Chem* **268**, 6995–7010.
17 Olson JS and Phillips GN Jr (1996) Kinetic pathways and barriers for ligand binding to myoglobin. *J Biol Chem* **271**, 17593–17596.
18 Andersen JF, Ding XD, Balfour C, Shokhireva TK, Champagne DE, Walker FA and Montfort WR (2000) Kinetics and equilibria in ligand binding by nitrophorins 1-4: evidence for stabilization of a nitric oxide-ferriheme complex through a ligand-induced conformational trap. *Biochemistry* **39**, 10118–10131.
19 Montfort WR, Weichsel A and Andersen JF (2000) Nitrophorins and related antihemostatic lipocalins from *Rhodnius prolixus* and other blood-sucking arthropods. *Biochim Biophys Acta* **1482**, 110–118.
20 Andersen JF (2010) Structure and mechanism in salivary proteins from blood-feeding arthropods. *Toxicon* **56**, 1120–1129.
21 De Simone G, Ascenzi P, di Masi A and Polticelli F (2017) Nitrophorins and nitrobindins: structure and function. *Biomol Concepts* **8**, 105–118.
22 Bianchetti CM, Blouin GC, Bitto E, Olson JS and Phillips GN Jr (2010) The structure and NO binding properties of the nitrophorin-like heme-binding protein from *Arabidopsis thaliana* gene locus At1 g79260.1. *Proteins* **78**, 917–931.
23 Bianchetti CM, Bingman CA and Phillips GN Jr (2011) Structure of the *C*-terminal heme-binding domain of THAP domain containing protein 4 from *Homo sapiens*. *Proteins* **79**, 1337–1341.
24 De Simone G, Ascenzi P and Polticelli F (2016) Nitrobindin: an ubiquitous family of all β-Barrel heme-proteins. *IUBMB Life* **68**, 423–428.
25 Larsson J, Allhorn M and Åkerström B (2004) The lipocalin α1-microglobulin binds heme in different species. *Arch Biochem Biophys* **432**, 196–204.
26 Weichsel A, Maes EM, Andersen JF, Valenzuela JG, Shokhireva TKH, Walker FA and Montfort WR (2005) Heme-assisted *S*-nitrosation of a proximal thiolate in a nitric oxide transport protein. *Proc Natl Acad Sci USA* **102**, 594–599.
27 Olsson MG, Centlow M, Rutardóttir S, Stenfors I, Larsson J, Hosseini-Maaf B, Olsson ML, Hansson SR and Akerström B (2010) Increased levels of cell-free hemoglobin, oxidation markers, and the antioxidative heme scavenger α1-microglobulin in preeclampsia. *Free Radic Biol Med* **48**, 284–291.
28 Roussigne M, Kossida S, Lavigne AC, Clouaire T, Ecochard V, Glories A, Amalric F and Girard JP (2003) The THAP domain: a novel protein motif with similarity to the DNA-binding domain of P element transposase. *Trends Biochem Sci* **28**, 66–69.
29 Clouaire T, Roussigne M, Ecochard V, Mathe C, Amalric F and Girard JP (2005) The THAP domain of THAP1 is a large C2CH module with zinc-dependent sequence-specific DNA-binding activity. *Proc Natl Acad Sci USA* **102**, 6907–6912.
30 Antonini E and Brunori M (1971) *Hemoglobin and Myoglobin in their Reactions with Ligands*. North Holland Publishing Co, Amsterdam, London.
31 Goldstein S and Merényi G (2008) The chemistry of peroxynitrite: implications for biological activity. *Methods Enzymol* **436**, 49–61.
32 Goldstein S, Lind J and Merényi G (2005) Chemistry of peroxynitrites and peroxynitrates. *Chem Rev* **105**, 2457–2470.
33 Mehl M, Daiber A, Herold S, Shoun H and Ullrich V (1999) Peroxynitrite reaction with heme proteins. *Nitric Oxide* **3**, 142–152.
34 Shimanovich R and Groves JT (2001) Mechanisms of peroxynitrite decomposition catalyzed by FeTMPS, a bioactive sulfonated iron porphyrin. *Arch Biochem Biophys* **387**, 307–317.
35 Jensen MP and Riley DP (2002) Peroxynitrite decomposition activity of iron porphyrin complexes. *Inorg Chem* **41**, 4788–4797.
36 Herold S and Shivashankar K (2003) Metmyoglobin and methemoglobin catalyze the isomerization of peroxynitrite to nitrate. *Biochemistry* **42**, 14036–14046.
37 Herold S, Exner M and Boccini F (2003) The mechanism of the peroxynitrite-mediated oxidation of myoglobin in the absence and presence of carbon dioxide. *Chem Res Toxicol* **16**, 390–402.

38 Herold S, Kalinga S, Matsui T and Watanabe Y (2004) Mechanistic studies of the isomerization of peroxynitrite to nitrate catalyzed by distal histidine metmyoglobin mutants. *J Am Chem Soc* **126**, 6945–6955.
39 Ascenzi P, di Masi A, Coletta M, Ciaccio C, Fanali G, Nicoletti FP, Smulevich G and Fasano M (2009) Ibuprofen impairs allosterically peroxynitrite isomerization by ferric human serum heme-albumin. *J Biol Chem* **284**, 31006–31017.
40 Ascenzi P, Ciaccio C, Sinibaldi F, Santucci R and Coletta M (2011) Cardiolipin modulates allosterically peroxynitrite detoxification by horse heart cytochrome *c*. *Biochem Biophys Res Commun* **404**, 190–194.
41 Ascenzi P, Ciaccio C, Sinibaldi F, Santucci R and Coletta M (2011) Peroxynitrite detoxification by horse heart carboxymethylated cytochrome *c* is allosterically modulated by cardiolipin. *Biochem Biophys Res Commun* **415**, 463–467.
42 Ascenzi P, Coletta A, Cao Y, Trezza V, Leboffe L, Fanali G, Fasano M, Pesce A, Ciaccio C, Marini S *et al*. (2013) Isoniazid inhibits the heme-based reactivity of *Mycobacterium tuberculosis* truncated hemoglobin N. *PLoS ONE* **8**, e69762.
43 Coppola D, Giordano D, Tinajero-Trejo M, di Prisco G, Ascenzi P, Poole RK and Verde C (2013) Antarctic bacterial haemoglobin and its role in the protection against nitrogen reactive species. *Biochim Biophys Acta* **1834**, 1923–1931.
44 Ascenzi P, Leboffe L, Pesce A, Ciaccio C, Sbardella D, Bolognesi M and Coletta M (2014) Nitrite-reductase and peroxynitrite isomerization activities of *Methanosarcina acetivorans* protoglobin. *PLoS ONE* **9**, e95391.
45 Ascenzi P, Leboffe L, Santucci R and Coletta M (2015) Ferric microperoxidase-11 catalyzes peroxynitrite isomerization. *J Inorg Biochem* **144**, 56–61.
46 Ascenzi P and Pesce A (2017) Peroxynitrite scavenging by *Campylobacter jejuni* truncated hemoglobin P. *J Biol Inorg Chem* **22**, 1141–1150.
47 Pfeiffer S, Gorren AC, Schmidt K, Werner ER, Hansert B, Bohle DS and Mayer B (1997) Metabolic fate of peroxynitrite in aqueous solution: reaction with nitric oxide and pH-dependent decomposition to nitrite and oxygen in a 2:1 stoichiometry. *J Biol Chem* **272**, 3465–3470.
48 Herold S, Matsui T and Watanabe Y (2001) Peroxynitrite isomerization catalyzed by His64 myoglobin mutants. *J Am Chem Soc* **123**, 4085–4086.
49 Miranda KM, Espey MG and Wink DA (2001) A rapid, simple spectrophotometric method for simultaneous detection of nitrate and nitrite. *Nitric Oxide* **5**, 62–71.
50 Takano T (1984) *Refinement of Myoglobin and Cytochrome c. Methods and Applications in Crystallographic Computing*, pp. 262-272. Oxford University Press, Oxford.
51 Milani M, Pesce A, Ouellet Y, Ascenzi P, Guertin M and Bolognesi M (2001) *Mycobacterium tuberculosis* hemoglobin N displays a protein tunnel suited for O_2 diffusion to the heme. *EMBO J* **20**, 3902–3909.
52 Nardini M, Pesce A, Thijs L, Saito JA, Dewilde S, Alam M, Ascenzi P, Coletta M, Ciaccio C, Moens L *et al*. (2008) Archaeal protoglobin structure indicates new ligand diffusion paths and modulation of haem-reactivity. *EMBO Rep* **9**, 157–163.
53 Pesce A, Tilleman L, Dewilde S, Ascenzi P, Coletta M, Ciaccio C, Bruno S, Moens L, Bolognesi M and Nardini M (2011) Structural heterogeneity and ligand gating in ferric *Methanosarcina acetivorans* protoglobin mutants. *IUBMB Life* **63**, 287–294.
54 Giordano D, Pesce A, Boechi L, Bustamante JP, Caldelli E, Howes BD, Riccio A, di Prisco G, Nardini M, Estrin D *et al*. (2015) Structural flexibility of the heme cavity in the cold-adapted truncated hemoglobin from the Antarctic marine bacterium *Pseudoalteromonas haloplanktis* TAC125. *FEBS J* **282**, 2948–2965.
55 Banci L, Bertini I, Gray HB, Luchinat C, Reddig T, Rosato A and Turano P (1997) Solution structure of oxidized horse heart cytochrome *c*. *Biochemistry* **36**, 9867–9877.
56 Banci L, Bertini I, Huber JG, Spyroulias GA and Turano P (1999) Solution structure of reduced horse heart cytochrome *c*. *J Biol Inorg Chem* **4**, 21–31.
57 Fanali G, di Masi A, Trezza V, Marino M, Fasano M and Ascenzi P (2012) Human serum albumin: from bench to bedside. *Mol Aspects Med* **33**, 209–290.
58 Shimizu H, Park S, Lee D, Shoun H and Shiro Y (2000) Crystal structures of cytochrome P450nor and its mutants (Ser286→Val, Thr) in the ferric resting state at cryogenic temperature: a comparative analysis with monooxygenase cytochrome P450s. *J Inorg Biochem* **81**, 191–205.
59 Nardini M, Pesce A, Labarre M, Richard C, Bolli A, Ascenzi P, Guertin M and Bolognesi M (2006) Structural determinants in the group III truncated hemoglobin from *Campylobacter jejuni*. *J Biol Chem* **281**, 37803–37812.
60 Lu C, Egawa T, Wainwright LM, Poole RK and Yeh SR (2007) Structural and functional properties of a truncated hemoglobin from a food-borne pathogen *Campylobacter jejuni*. *J Biol Chem* **282**, 13627–13636.
61 Bolli A, Ciaccio C, Coletta M, Nardini M, Bolognesi M, Pesce A, Guertin M, Visca P and Ascenzi P (2008) Ferrous *Campylobacter jejuni* truncated hemoglobin P displays an extremely high reactivity for cyanide - a comparative study. *FEBS J* **275**, 633–645.
62 Dioum EM, Rutter J, Tuckerman JR, Gonzalez G, Gilles-Gonzalez MA and McKnight SL (2002) NPAS2: a gas-responsive transcription factor. *Science* **298**, 2385–2387.
63 Ascenzi P, Bocedi A, Leoni L, Visca P, Zennaro E, Milani M and Bolognesi M (2004) CO sniffing through heme-based sensor proteins. *IUBMB Life* **56**, 309–315.

64 Pettersen EF, Goddard TD, Huang CC, Couch GS, Greenblatt DM, Meng EC and Ferrin TE (2004) UCSF Chimera - a visualization system for exploratory research and analysis. *J Comput Chem* **25**, 1605–1612.

Supporting information

Additional supporting information may be found online in the Supporting Information section at the end of the article.

Fig. S1. Absorbance spectra of human Nb(III) and Nb (III)-NO (T = 25.0 °C). (A) Absorbance spectra of human Nb(III) at pH 6.1 (spectrum a) and 7.8 (spectrum b). For clarity, the absorbance spectrum obtained at pH 7.8 has been up-shifted of 0.5 units. (B) Absorbance spectra of human Nb(III) (continuous line) and Nb(III)-NO (dashed line) at pH 7.4. The λ_{max} values of human Nb(III) and Nb(III)-NO are 406 and 412 nm, respectively.